Coherent transfer of orbital angular momentum from an atomic system to a light field

Daisuke Akamatsu and Mikio Kozuma*
Department of Physics, Tokyo Institute of Technology, 2-12-1 O-okayama, Meguro-ku, Tokyo 152-8550, Japan
(Received 4 February 2002; published 6 February 2003)

We generated orbital angular momentum in atoms with a spin degree of freedom and coherently transferred it to a light field, which resulted in the generation of a Laguerre-Gaussian (LG) beam. In this method, atoms obtain orbital angular momentum through Larmor precession around the quadrupole field. Successive operations of quadrupole and homogeneous magnetic fields lead to a change of sign in the LG beam or even generation of superposition states of the LG beam with different indexes in real time. Possible applications to control orbital angular momentum of arbitrary photons are also discussed.

DOI: 10.1103/PhysRevA.67.023803 PACS number(s): 42.50.Gy, 03.67.−a

I. INTRODUCTION

The Laguerre-Gaussian (LG) mode is an eigenmode of the paraxial wave equation [1], whose unique properties are now attracting considerable attention in various research areas. Its doughnutlike intensity profile is suitable for trapping cold atoms [2]. The discrete orbital angular momentum of photons in the LG mode can be utilized for generating multidimensionally entangled states [3–5]. Due to the phase singularity, the LG beam is often called an optical vortex, and recent observation of the dynamic inversion of its topological charge is providing deep insights into other vortices [6]. Generally, an LG beam is generated by using computer-generated holograms [7–9], spiral or nonspiral phase plates [10,11], mode converters [12], and so on. The most frequently used and robust methods are, we believe, computer-generated holograms and phase plates.

Here we report a method for generating LG beams. Atomic spins are rotated around a quadrupole magnetic field, and the generated spatially varying quantum phase was transferred to a light field, which resulted in the generation of an LG beam. The interaction rate between atomic spin and the applied magnetic field can be easily increased by just increasing the field intensity, and thus real-time control of LG beams becomes possible [13]. Note that the mechanical orbital angular momentum of the LG beam has already been confirmed experimentally through observation of the rotation of micro-objects irradiated by an LG beam [14–16]. Therefore, our result proves that the quantum phase given by a quadrupole magnetic field leads to the mechanical orbital angular momentum even for atomic systems. In this sense, our experimental result verifies the validity of the recently proposed idea for creating vortices in an atomic gas Bose-Einstein condensate [17].

In this paper, we first theoretically present how to generate LG beams through interaction between atomic spins and magnetic fields. We also clarify that successive operations of quadrupole and homogeneous magnetic fields change the sign of an LG beam or even generate superposition states of LG beams with different indexes. In the following section, we present experimental results on generation of LG beams by using a simple rubidium vapor cell filled with ^{4}He buffer gas. Control of the sign and generation of superposition states are also demonstrated. Finally, we discuss possible applications for manipulating orbital angular momentum for single photons by combining our method with the recently proposed and demonstrated ''storage of light'' technique [18–21].

II. THEORY

A. Generation of the LG beam

We consider a spin-1 atomic system [Fig. 1(a)], where eigenstates (Zeeman sublevels) along the z axis are given by

$$|m_z=1\rangle=\begin{pmatrix}1\\0\\0\end{pmatrix},\quad |m_z=0\rangle=\begin{pmatrix}0\\1\\0\end{pmatrix},\quad |m_z=-1\rangle=\begin{pmatrix}0\\0\\1\end{pmatrix}. \tag{1}$$

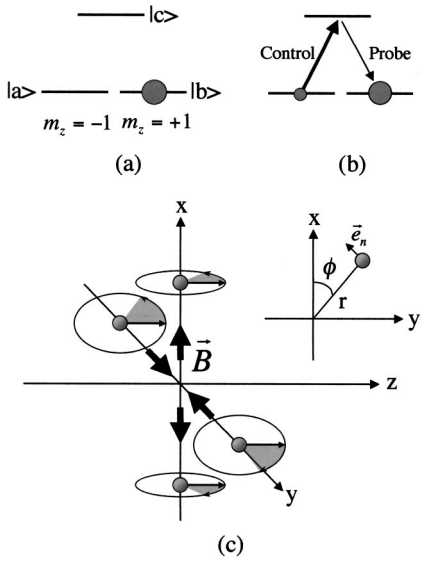

FIG. 1. (a) Atoms are initially pumped to the $|b\rangle$ state. (b) Spin coherence is generated by Larmor precession. A probe beam is generated by applying the control beam. (c) Time evolution of atomic spin in a quadrupole magnetic field.

*FAX: +81-3-5734-2451. Email address: kozuma@ap.titech.ac.jp

 ©2003 The American Physical Society

We express the unit vector on the xy plane as $\vec{e}_n=\cos(\theta)\vec{e}_x+\sin(\theta)\vec{e}_y$. On this basis, the Larmor precession of atomic spin along magnetic field $\vec{B}=B\vec{e}_n$ is expressed as

$$R(\omega\Delta t)=\begin{pmatrix} \frac{1}{2}(1+\cos\omega\Delta t) & -\frac{i}{\sqrt{2}}e^{-i\theta}\sin\omega\Delta t & -\frac{1}{2}e^{-2i\theta}(1-\cos\omega\Delta t) \\ -\frac{i}{\sqrt{2}}e^{i\theta}\sin\omega\Delta t & \cos\omega\Delta t & -\frac{i}{\sqrt{2}}e^{-i\theta}\sin\omega\Delta t \\ -\frac{1}{2}e^{2i\theta}(1-\cos\omega\Delta t) & -\frac{i}{\sqrt{2}}e^{i\theta}\sin\omega\Delta t & \frac{1}{2}(1+\cos\omega\Delta t) \end{pmatrix}. \tag{2}$$

Here, ω is the Larmor frequency, $\omega=g\mu_B B/\hbar$, and Δt is the precession time. g is the Lande factor and μ_B is the Bohr magneton. By substituting $\theta=0$ into Eq. (2), we obtain the matrix representation R_x for Larmor precession due to a homogeneous magnetic field along the x axis. The quadrupole magnetic field at point (r,ϕ) is represented by $\vec{e}_n=\cos(\phi)\vec{e}_x-\sin(\phi)\vec{e}_y$ and $B=B_r r$, where $B_r=\partial B/\partial r$ [see Fig. 1(c)]. Substituting $\theta=-\phi$, matrix representation R_q, which represents spin precession around a quadrupole field, is obtained as follows:

$$R_x(\omega\Delta t)=\begin{pmatrix} \frac{1}{2}(1+\cos\omega\Delta t) & -\frac{i}{\sqrt{2}}\sin\omega\Delta t & -\frac{1}{2}(1-\cos\omega\Delta t) \\ -\frac{i}{\sqrt{2}}\sin\omega\Delta t & \cos\omega\Delta t & -\frac{i}{\sqrt{2}}\sin\omega\Delta t \\ -\frac{1}{2}(1-\cos\omega\Delta t) & -\frac{i}{\sqrt{2}}\sin\omega\Delta t & \frac{1}{2}(1+\cos\omega\Delta t) \end{pmatrix}, \tag{3a}$$

$$R_q(\omega\Delta t)=\begin{pmatrix} \frac{1}{2}(1+\cos\omega\Delta t) & -\frac{i}{\sqrt{2}}e^{i\phi}\sin\omega\Delta t & -\frac{1}{2}e^{2i\phi}(1-\cos\omega\Delta t) \\ -\frac{i}{\sqrt{2}}e^{-i\phi}\sin\omega\Delta t & \cos\omega\Delta t & -\frac{i}{\sqrt{2}}e^{i\phi}\sin\omega\Delta t \\ -\frac{1}{2}e^{-2i\phi}(1-\cos\omega\Delta t) & -\frac{i}{\sqrt{2}}e^{-i\phi}\sin\omega\Delta t & \frac{1}{2}(1+\cos\omega\Delta t) \end{pmatrix}. \tag{3b}$$

Atoms are initially pumped into the $|m_z=1\rangle$ state. Applying magnetic field $\vec{B}=B\vec{e}_n$ during Δt, the atomic spin precesses and the state evolutes as

$$|\psi(\omega\Delta t)\rangle=R(\omega\Delta t)\begin{pmatrix}1\\0\\0\end{pmatrix}=\begin{pmatrix} \frac{1}{2}(1+\cos\omega\Delta t) \\ -\frac{i}{\sqrt{2}}e^{i\theta}\sin\omega\Delta t \\ -\frac{1}{2}e^{2i\theta}(1-\cos\omega\Delta t) \end{pmatrix}. \tag{4}$$

Therefore, the coherence generated between $|m_z=-1\rangle$ and $|m_z=1\rangle$ states [$|a\rangle$ and $|b\rangle$ in Fig. 1(a)] is given by

$$\rho_{ab}=-\frac{1}{4}\sin^2\omega\Delta t\exp(-2i\theta). \tag{5}$$

In this paper, we call this spin coherence. When atoms are irradiated by control light in Gaussian mode corresponding to the $|a\rangle\leftrightarrow|c\rangle$ transition for $\Delta\tau$, polarization P_{bc} proportional to $\rho_{ab}\Omega_c\Delta\tau$ is generated between $|b\rangle$ and $|c\rangle$ states, where Ω_c represents the single-photon Rabi frequency of the control beam:

$$P_{bc}\propto\exp(-r^2/w_0^2)\exp(-2i\theta)[\sin^2(\omega\Delta t)\Delta\tau]. \tag{6}$$

Here, w_0 represents the beam waist of the control beam. This polarization generates a probe beam corresponding to $|b\rangle \leftrightarrow |c\rangle$ transition [Fig. 1(b)]. When a homogeneous magnetic field is applied along the x axis, successive irradiation of control light generates polarization of

$$P_{bc} \propto \exp(-r^2/w_0^2)[\sin^2(\omega\Delta t)\Delta\tau]. \tag{7}$$

This means the generated probe beam has the same Gaussian intensity profile. In a quadrupole magnetic field, the polarization within the range of $r \ll \hbar/(g\mu_B B_r \Delta t)$ is given by

$$P_{bc} \propto r^2 \exp(-r^2/w_0^2)\exp(2i\phi)\Delta\tau(\Delta t)^2. \tag{8}$$

Equation (8) reveals that the electric field of the probe beam is exactly equal to that of the second-order LG beam. In other words, the photon constituting the probe beam possesses an orbital angular momentum of $2\hbar$. Atoms receive spatially varying quantum phase through Larmor precession around a quadrupole field, which leads to the mechanical orbital angular momentum of the system. This mechanical orbital angular momentum is coherently transferred to the probe beam.

B. Control of the sign of the LG beam

Here, we consider how to change the sign of the LG beam. As can be seen from Eq. (8), the sign of the LG beam does not depend on the direction of the current flowing in the quadrupole coil. The following successive operations of R_x and R_q are required to generate an LG beam with a negative index:

$$|\psi(\omega\Delta t)\rangle = R_x(\pi)R_q(\omega\Delta t)R_x(\pi)\begin{pmatrix}1\\0\\0\end{pmatrix} = \begin{pmatrix} \frac{1}{2}(1+\cos\omega\Delta t) \\ -\frac{i}{\sqrt{2}}e^{i\phi}\sin\omega\Delta t \\ -\frac{1}{2}e^{2i\phi}(1-\cos\omega\Delta t)\end{pmatrix}. \tag{9}$$

Here, for comparison, we give the spin state only after the quadrupole operation is performed, i.e.,

$$|\psi(\omega\Delta t)\rangle = R_q(\omega\Delta t)\begin{pmatrix}1\\0\\0\end{pmatrix} = \begin{pmatrix} \frac{1}{2}(1+\cos\omega\Delta t) \\ -\frac{i}{\sqrt{2}}e^{-i\phi}\sin\omega\Delta t \\ -\frac{1}{2}e^{-2i\phi}(1-\cos\omega\Delta t)\end{pmatrix}. \tag{10}$$

We find that only the sign for azimuthal angle ϕ is different between Eqs. (9) and (10). Magnetic operations given by Eq. (9) generate spin coherence $\rho_{ab} \propto \exp(-2i\phi)$. One can thus obtain an LG beam with a negative index.

C. Generation of superposition states

Next, we consider how to generate the superposition state of LG beams with different indexes. After Larmor precession around a quadrupole field, we apply a homogeneous magnetic field along the x axis. The atomic spin state after these operations is given by

$$|\psi(\Delta t)\rangle = R_x(\theta_x)R_q(\theta_q)\begin{pmatrix}1\\0\\0\end{pmatrix} = \begin{pmatrix} \frac{1}{4}\{(1-\cos\theta_q)(1-\cos\theta_x)e^{-2i\phi} - 2\sin(\theta_q)\sin(\theta_x)e^{-i\phi} + (1+\cos\theta_q)(1+\cos\theta_x)\} \\ \frac{i}{2\sqrt{2}}\{(1-\cos\theta_q)\sin(\theta_x)e^{-2i\phi} - 2\sin(\theta_q)\cos(\theta_x)e^{-i\phi} - (1+\cos\theta_q)\sin\theta_x\} \\ \frac{1}{4}\{-(1-\cos\theta_q)(1+\cos\theta_x)e^{-2i\phi} - 2\sin(\theta_q)\sin(\theta_x)e^{-i\phi} - (1+\cos\theta_q)(1-\cos\theta_x)\}\end{pmatrix}, \tag{11}$$

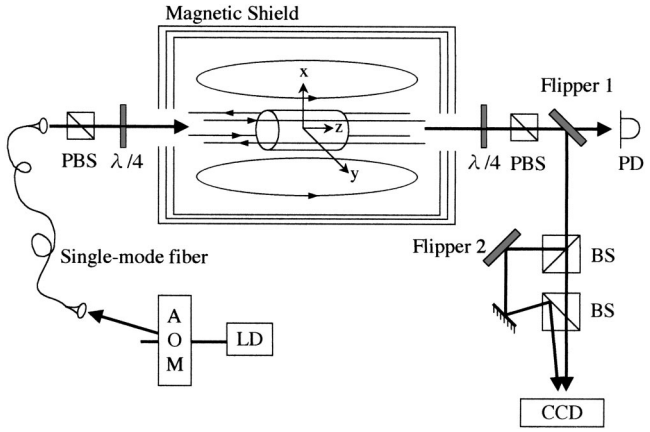

FIG. 2. Schematic explanation of the experimental setup. PBS: polarizing beam splitter. BS: beam splitter. λ/4: λ/4 plate. LD: laser diode. AOM: acousto-optic modulator. PD: photodetector.

where θ_x and θ_q are precession angles. Spin coherence is thus given by

$$\begin{aligned}\rho_{ab} \propto & -(1+\cos\theta_x)^2 \sin^2(\theta_q) e^{2i\phi} - 2(1+\cos\theta_x) \\ & \times \sin(2\theta_q)\sin(\theta_x) e^{i\phi} + 2(1-3\cos^2\theta_q)\sin^2\theta_x \\ & + 2(1-\cos\theta_x)\sin(2\theta_q)\sin(\theta_x) e^{-i\phi} \\ & - (1-\cos\theta_x)^2 \sin^2(\theta_q) e^{-2\phi}. \end{aligned} \tag{12}$$

We find that the generated probe light is in the superposition state of LG modes with mode indexes from -2 to $+2$. This result can be explained qualitatively. As can be seen from Eq. (10), the $|m_z=i\rangle$ spin component $(i=-1,0,+1)$ acquires variation of the quantum phase around the azimuthal angle ϕ, which is proportional to $\Delta m_z = i-1$, through Larmor precession around a quadrupole magnetic field. Successive application of a homogeneous magnetic field coherently mixes these spin components. Both $|m_z=\pm 1\rangle$ states thus obtain phase variations of $e^{-i\phi}$ and $e^{-2i\phi}$. When the order of operation for R_x and R_q is exchanged, superposition states with mode indexes from 0 to 4 are generated. Note that by repeating the set of operations, one can generate superposition states with higher indexes.

III. EXPERIMENT

A. Generation of the LG beam

Our experiment was carried out in a pure ^{87}Rb vapor cell filled with 5 torr of ^{4}He buffer gas (Fig. 2). The 10-cm-long, 30-mm-diameter cell was magnetically shielded by threefold permalloy, and its temperature was actively stabilized to 50 °C with a nonmagnetic wire, which corresponds to an atomic density of 1.4×10^{11} cm^{-3}. We employed the D_1 line $5\ ^2S_{1/2},\ F=2 \rightarrow 5\ ^2P_{1/2},\ F=1$ transition (795 nm). Here, $|F=2,m_z=0\rangle$, $|F=2,m_z=2\rangle$, and $|F'=1,m_z=1\rangle$ correspond to $|a\rangle$, $|b\rangle$, and $|c\rangle$, respectively. Inside the magnetic shield, two coils were installed to generate homogeneous and quadrupole magnetic fields.

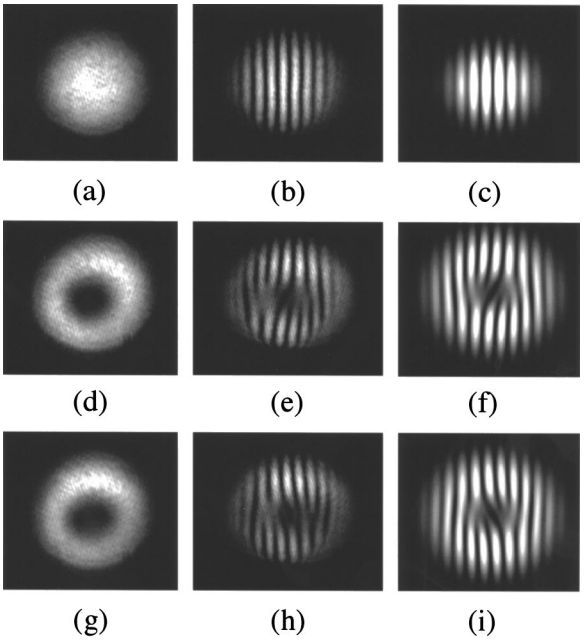

FIG. 3. (a),(d),(g) Intensity profiles of generated probe beams. (b),(e),(h) Interference patterns of the generated probe beams. (c),(f),(i) Numerical simulations.

The intensity of the control beam derived from an extended cavity diode laser was controlled by using an acousto-optic modulator. The spatial mode of the beam was purified by using a single-mode fiber, where the beam waist and total power were 3 mm and 1 mW. Applying a circularly polarized (σ^+) control beam for 10 ms pumped atoms to the $|F=2,m_z=2\rangle$ state. After the control beam was turned off, we applied a homogeneous magnetic pulse along the x axis for 30 μs, which corresponded to a $\pi/2$ pulse. As a result, the spin coherence expressed by Eq. (5) was generated between the $|F=2,m_z=2\rangle$ and $|F=2,m_z=0\rangle$ states. By turning the control beam on again, we could generate a circularly polarized (σ^-) probe beam. Only the probe beam passed through the λ/4 plate and polarizing beam splitter, and its intensity was monitored by a photodetector. The peak power of the generated probe beam was 70 μW, and its pulse length, 20 μs. Note that the spin coherence was maintained for more than 100 μs because of the magnetic shields and the ^{4}He buffer gas [22]. By using Flipper 1, we also monitored the spatial profile of the probe beam with a charge-coupled device camera. As shown in Fig. 3(a), the probe beam had a Gaussian profile identical to that of the control beam. By using Flipper 2, we overlapped two probe beams split by a beam splitter with a small crossing angle. As discussed later, when the beam has orbital angular momentum, the fringe pattern exhibits a forking structure. The observed image [Fig. 3(c)] did not exhibit such a forking pattern.

Next, we applied a quadrupole magnetic field for 30 μs after the optical pumping stage. The applied magnetic field corresponded to a $\pi/2$ pulse at the position of laser beam waist. When we turned the control beam on, a probe beam with a power of 30 μW was generated for 20 μs. The probe beam had a doughnutlike spatial profile [Fig. 3(b)]. The doughnutlike intensity profile does not necessarily mean the

probe beam has phase singularity. The best way to check the phase singularity is to observe the interference pattern by overlapping the probe beam with a tilted plane wave. Because the phase of the probe beam varies by $2n\pi$ (n is an integer) around the beam center, dark (bright) lines in a fringe pattern vanish at the center of the beam, i.e., the forking fringe pattern appears. The number of dark (bright) lines that vanish at the center represents the index of the LG beam. In our experiment, we overlapped the probe beam with its copy for convenience [23,24]. When the beam centers are separated enough compared to the fringe spacing, one probe beam serves roughly as a plane wave for the other beam. Eventually, one can see two forking fringe patterns. The fringe pattern obtained by our experiment clearly exhibited such a forking structure [Fig. 3(e)], which agrees well with the simulation [Fig. 3(f)] for the second order of the LG beam. From Eq. (4), the order of the generated LG beam depends only on the difference of spin between the two ground states $|1\rangle$ and $|2\rangle$, i.e., $\Delta m_z=2$. We varied the magnitude of the applied magnetic field within the range of $r \ll \hbar/(g\mu_B B_r \Delta t)$ and checked the order of the LG beam by using the interference method. The order did not change, but the total intensity did. Note that our theory is constructed for the spin-1 system, while the experiment was performed for the spin-2 system. Transition strength for $|F=1,m_z=1\rangle \Leftrightarrow |F'=1,m_z=0\rangle$ ($|F=1,m_z=1\rangle \Leftrightarrow |F'=2,m_z=0\rangle$) is much weaker than that for $|F=2,m_z=2\rangle \Leftrightarrow |F'=1,m_z=1\rangle$, which decreases probe signal intensity and thus we did not employ $F=1$ ground state. While the experiment was performed for the spin-2 system, the experimental results were well explained by our theory, which was because only three Zeeman sublevels, i.e., $|F=2,m_z=2\rangle$, $|F=2,m_z=0\rangle$, and $|F'=1,m_z=1\rangle$, mainly contributed to the signal generation.

B. Control of the sign of the LG beam

Next, we generated an LG beam with a negative index based on the magnetic operation depicted by Eq. (9). We first optically pumped atoms to the $|F=2,m_z=2\rangle$ state using the control beam. Applying a homogeneous magnetic field along the x axis rotated the atomic spin in π, i.e., the spin state was converted to $|F=2,m_z=-2\rangle$. After generating the spin coherence between $|F=2,m_z=-2\rangle$ and $|F=2,m_z=0\rangle$ with a quadrupole field, we rotated the spin in π again with a homogeneous magnetic field. Eventually, the spin coherence between $|F=2,m_z=-2\rangle$ and $|F=2,m_z=0\rangle$ was converted to that between $|F=2,m_z=2\rangle$ and $|F=2,m_z=0\rangle$, which is proportional to $\exp(-2i\phi)$. Turning the control beam on again generated an LG beam with a negative index. The experimentally observed spatial profile and interference pattern of the probe beam are shown in Figs. 3(g) and 3(h). The intensity profile had the same doughnutlike shape, but the interference pattern was upside down, which is a clear evidence of an LG beam with a negative index.

C. Generation of superposition states

Finally, we generated superposition states of LG beams with different indexes. First, applying a homogeneous magnetic field for 30 μs rotated atoms in the $|F=2,m_z=2\rangle$ state by an angle of ξ_x around the x axis. Next, we applied a quadrupole magnetic field corresponding to a $\pi/2$ pulse for 30 μs. Figure 4(a) shows intensity profiles of probe beams generated by turning the control beam on (from the top $\xi_x=0$, $\pi/4$, $\pi/2$, $3\pi/4$, and π). The images appeared to rotate around the y axis as angle ξ_x increased. Figure 4(b) shows the numerical results of spatial profiles of the probe beams calculated based on induced polarization. Experimental results are in good agreement with simulations. Figure 4(c) displays the square of the coefficient in expanding the probe field by the LG mode. One can find out that generated probe beams were superposition states of LG modes with mode indexes from 0 to 4, as was discussed in Sec. II C. The experimental result for $\xi_x=\pi$ [bottom of Fig. 4(a)] has two dark spots, while the numerical result has only one spot [bottom of Fig. 4(b)]. We experimentally determined that the phase of the electric field changed by 2π around each of these two dark spots. This is the superposition state of Gaussian and the second-order LG beams, which is different from the simulation [see bottom of Fig. 4(c)] [25]. Optical pumping could not be perfect because of the hot atomic sample, i.e., atoms were partially pumped to $|F=2,m_z=1\rangle$, not $|F=2,m_z=2\rangle$. While atoms in $|F=2,m_z=2\rangle$ were ro-

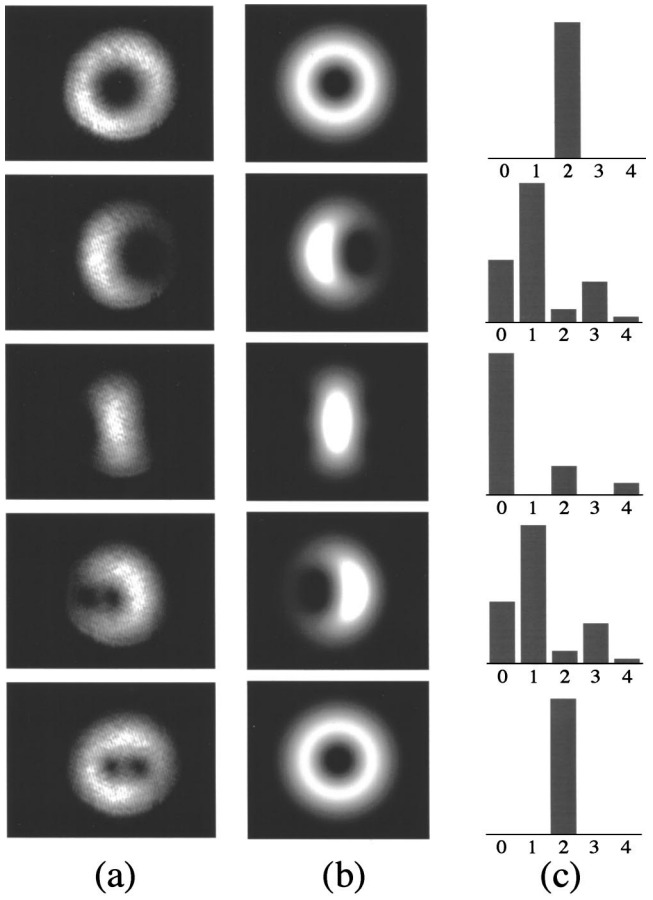

FIG. 4. (a) Intensity profile of the probe beam generated by successively applying the homogeneous and quadrupole magnetic fields. The horizontal and vertical lines correspond to x and y axes. (b) Simulations of probe beam intensity profiles. (c) The square of the coefficient in expanding the probe field by the LG mode.

tated in $\xi_x=\pi$ by applying a homogeneous field, atoms in $|F=2,m_z=1\rangle$ were rotated in $\pi/2$, which created spin coherence between $|F=2,m_z=1\rangle$ and $|F=2,m_z=-1\rangle$ states. Eventually, when the control beam was turned on, both a second-order LG beam and a Gaussian beam were generated.

IV. DISCUSSION

Recently, it was theoretically shown that quantum information of light can be perfectly transferred to coherence between different spin states of atoms [18,19]. Preliminary experiments have also been carried out with sodium and rubidium atoms [20,21]. An interesting application of this storage and retrieval of light method is manipulating stored photonic information. Because all photonic information is converted to atomic spin coherence, the information can be easily manipulated through electromagnetic interactions. In fact, the relative phase between the control and retrieved optical pulses was successfully controlled by applying a homogeneous magnetic field along the optical axis [26]. The pulse length of the retrieved light was also controlled by changing the intensity of the control light [21].

Here, we discuss the possibility of controlling orbital angular momentum of arbitrary photons by combining our method with the storage and retrieval of light technique. In the storage and retrieval of light technique, coherent light is stored as a coherent state of collective atomic spins. Even if the light is in a nonclassical state like squeezed light, photonic information can be stored as a spin-squeezed state [27–29], where atoms are correlated with each other in a nonlocal manner. In principle, single photons can be stored in atomic medium. One can give an atomic system a spatially varying quantum phase through magnetic interaction after information of a single photon is transferred to purely atomic information. By applying the control beam again, one can retrieve the stored photon that now has orbital angular momentum. Here, we will briefly discuss such a possibility based on the dark-state polariton concept established by Fleischhauer and Lukin [18,19].

Propagation of an electromagnetic field in an atomic medium is well described as a mixture of electromagnetic and collective atomic excitations of spin transitions, i.e., dark-state polaritons. When the electric field and the atomic spin coherence are represented by $\hat{\varepsilon}(z,t)$ and $\hat{\sigma}_{ab}(z,t)$, the dark-state polariton is given by

$$\hat{\psi}(z,t)=\cos\theta(t)\hat{\varepsilon}(z,t)-\sin\theta(t)\sqrt{N}\hat{\sigma}_{ab}(z,t), \quad (13)$$

where

$$\tan\theta(t)=\frac{g\sqrt{N}}{\Omega_c(t)}. \quad (14)$$

Here, θ and N are the mixing angle and the number of atoms involved. Introducing a plane-wave decomposition $\hat{\psi}(z,t)=\Sigma_k\hat{\psi}_k(t)e^{ikz}$, mode operators obey the following commutation relations when the photon number density is much smaller than the atomic density,

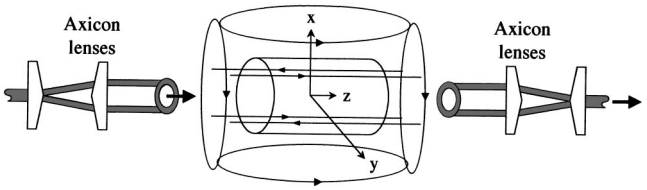

FIG. 5. Setup for manipulating the orbital angular momentum of the stored light field. The spatial profile of injected light is converted to a ring type by using axicon lenses. After passing through an atomic medium, the beam profile is again converted to the original Gaussian mode.

$$[\hat{\psi}_k,\hat{\psi}_k]=\delta_{k,\kappa}. \quad (15)$$

Let us consider the situation in which a single photon is injected into the atomic medium. This state is described as

$$\hat{a}_k^+|0\rangle|b_1\cdots b_N\rangle=|1\rangle|b_1\cdots b_N\rangle. \quad (16)$$

Here, $|b_1\cdots b_N\rangle$ means N atoms are in spin state $|b\rangle$ in Fig. 1(a). Adiabatically decreasing control light intensity converts the state to a purely atomic one, i.e.,

$$\hat{\sigma}_{ab}^+|0\rangle|b_1\cdots b_N\rangle=|0\rangle\frac{1}{\sqrt{N}}\sum_{j=1}^{N}|b_1\cdots a_j\cdots b_N\rangle. \quad (17)$$

After storing a single photon, we perform spin operation with a magnetic field. Note that the spatial profile of a single-photon source is originally converted to a ring type by using an axicon lens system (see Fig. 5), where only the spatial profile is changed and thus the photon does not obtain any orbital angular momentum. The ring profile is converted to a normal Gaussian mode after passing through an atomic medium. When magnetic operation is not performed, the process is reversed in a unitary manner and a single photon is retrieved by recovering the control light intensity.

Next, we consider the case where the following magnetic operations [see Fig. 6(a)] are performed after the storage stage [17], i.e.,

$$B_z=B_{z0}\cos\left[\pi\left(1-\frac{t}{T}\right)\right] \quad (18a)$$

and

$$B_q=B_r r\sin\left[\pi\left(1-\frac{t}{T}\right)\right]. \quad (18b)$$

For simplicity, we assume that the ring beam is narrow enough so that the magnetic field can be approximately uniform within the ring region, i.e., $B_{z0}=B_r r=B_0$. Here, we also assume the adiabatic condition $\omega_L T\gg 1$, where $\omega_L=g\mu_B B_0/\hbar$. Time evolution from 0 to T leads to a population exchange between $|a\rangle$ and $|b\rangle$ states, and a Berry phase appears between them. Note that this operation does not generate any additional spin coherence. After completing this procedure, we perform the following magnetic operation [see Fig. 6(b)]:

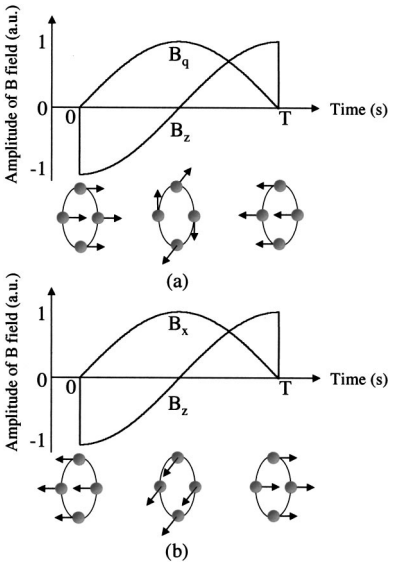

FIG. 6. Magnetic operations for inducing orbital angular momentum into the injected light field. Pictures under graphs are schematic illustrations of time evolutions of atomic spins. (a) Through interaction with quadrupole and homogeneous fields, atoms obtain Berry phase but spin direction is inverted. (b) By using homogeneous fields, atomic spin direction is inverted again.

$$B_z = B_0 \cos\left[\pi\left(1-\frac{t}{T}\right)\right] \tag{19a}$$

and

$$B_x = B_0 \sin\left[\pi\left(1-\frac{t}{T}\right)\right]. \tag{19b}$$

The population is again exchanged, and the spin coherence becomes

$$\hat{\sigma}_{ab}^{(\mathrm{Berry})}(z,t) = e^{i4\pi\varphi}\hat{\sigma}_{ab}(z,t), \tag{20}$$

where the Berry phase is determined by the spin difference between $|a\rangle$ and $|b\rangle$. A linear combination of $\hat{\sigma}_{ab}^{(\mathrm{Berry})}$ and $\hat{\varepsilon}^{(\mathrm{LG2})}(z,t) = e^{i4\pi\varphi}\hat{\varepsilon}(z,t)$, i.e.,

$$\hat{\psi}'(z,t) = \cos\theta(t)\hat{\varepsilon}^{(\mathrm{LG2})}(z,t) - \sin\theta(t)\sqrt{N}\hat{\sigma}_{ab}^{(\mathrm{Berry})}(z,t), \tag{21}$$

apparently satisfies the commutation relation in the same way as Eq. (15). Turning the control beam on again thus adiabatically converts the atomic state after magnetic operation,

$$\hat{\sigma}_{ab}^{(\mathrm{Berry})+}|0\rangle|b_1\cdots b_N\rangle = e^{i4\pi\varphi}|0\rangle\frac{1}{\sqrt{N}}\sum_{j=1}^{N}|b_1\cdots a_j\cdots b_N\rangle, \tag{22}$$

to

$$\hat{a}_k^{(\mathrm{LG2})+}|0\rangle|b_1\cdots b_N\rangle = e^{i4\pi\varphi}|1\rangle|b_1\cdots b_N\rangle. \tag{23}$$

Namely, it is possible to manipulate the orbital angular momentum of the injected single photon. This experiment is now being conducted at our laboratory.

V. SUMMARY

We gave an atomic gas sample a spatially varying quantum phase by using a spin degree of freedom, which led to mechanical orbital angular momentum of atoms. The generated orbital angular momentum was coherently transferred to a light field. In our method, a specific order of the LG beam can be selectively generated. Just by changing the magnetic pulse sequence, one can control the sign of an LG beam or even generate a superposition state of LG beams with different indexes in real time. Combining our method with the storage and retrieval of light technique will enable freely manipulating orbital angular momentum of arbitrary photons. It is very fascinating to consider storing twin photons in separate atomic samples and manipulating their orbital angular momenta. Such manipulation will be a powerful tool for quantum information processing with multidimensional entangled states for photons.

ACKNOWLEDGMENTS

We thank L. Deng, E. W. Hagley, M. Ueda, T. Kuga, S. Tomatsu, and T. Kawasaki for their valuable comments and many stimulating discussions. We also thank Sony Ltd. for supplying the laser diode. This work was supported by the program ''Research and Development on Quantum Communication Technology'' of the Ministry of Public Management, Home Affairs, Posts and Telecommunications of Japan, the Asahi Glasses Foundation, and the Matsuo Foundation.

[1] L. Allen, M. W. Beijersbergen, R. J. C. Sqreeuw, and J. P. Woerdman, Phys. Rev. A **45**, 8185 (1992).
[2] T. Kuga, Y. Torii, N. Shiokawa, T. Hirano, Y. Shimizu, and H. Sasada, Phys. Rev. Lett. **78**, 4713 (1997).
[3] A. Mair, A. Vaziri, G. Weihs, and A. Zeilinger, Nature (London) **412**, 313 (2001).
[4] H. H. Arnaut and G. A. Barbosa, Phys. Rev. Lett. **85**, 286 (2000).
[5] J. Arlt, K. Dholakia, L. Allen, and M. J. Padgett, Phys. Rev. A **59**, 3950 (1999).
[6] G. Molina-Terriza, J. Recolons, J. P. Torres, L. Torner, and E. M. Wright, Phys. Rev. Lett. **87**, 023902 (2001).
[7] V. Y. Bazhenov, M. V. Vasnetsov, and M. S. Soskin, Pis'ma Zh. Eksp. Teor. Fiz. **52**, 1037 (1990) [JETP Lett. **52**, 429 (1990)].
[8] N. R. Heckenberg, R. McDuff, C. P. Smith, and A. G. White, Opt. Lett. **17**, 221 (1992).
[9] J. Arlt, K. Dholakia, L. Allen, and M. J. Padgett, J. Mod. Opt. **45**, 1231 (1998).
[10] M. W. Beijersbergen, R. P. C. Coerwinkel, M. Kristensen, and J. P. Woerdman, Opt. Commun. **112**, 321 (1994).
[11] Guang-Hoon Kim, Jin-Ho Jeon, Kwang-Hoon Ko, Hee-Jong Moon, Jai-Hyung Lee, and Joon-Sung Chang, Appl. Opt. **36**,

8614 (1997).
[12] M. W. Beijersbergen, L. Allen, H. E. L. O. van der Veen, and J. P. Woerdman, Opt. Commun. **96**, 123 (1993).
[13] Reconfigurable hologram can be utilized for optical space switches. For example, see W. A. Crossland, I. G. Manolis, M. M. Redmond, K. L. Tan, T. D. Wilkinson, M. J. Holmes, T. R. Parker, H. H. Chu, J. Croucher, V. A. Handerek, S. T. Warr, B. Robertson, I. G. Bonas, R. Franklin, C. Stace, H. J. White, R. A. Woolley, and G. Henshall, J. Lightwave Technol. **LT18**, 1845 (2000).
[14] N. B. Simpson, K. Dholakia, L. Allen, and M. J. Padgett, Opt. Lett. **22**, 52 (1997).
[15] P. Galajda and P. Ormos, Appl. Phys. Lett. **78**, 249 (2001).
[16] M. E. J. Friese, J. Enger, H. Rubinsztein-Dunlop, and N. R. Heckenberg, Phys. Rev. A **54**, 1593 (1996).
[17] T. Isoshima, M. Nakahara, T. Ohmi, and K. Machida, Phys. Rev. A **61**, 063610 (2000).
[18] M. Fleischhauer and M. D. Lukin, Phys. Rev. Lett. **84**, 5094 (2000).
[19] M. Fleischhauer and M. D. Lukin, Phys. Rev. A **65**, 022314 (2002).
[20] D. F. Phillips, A. Fleischhauer, A. Mair, R. L. Walsworth, and M. D. Lukin, Phys. Rev. Lett. **86**, 783 (2001).
[21] C. Liu, Z. Dutton, C. H. Behroozi, and L. V. Hau, Nature (London) **409**, 490 (2001).
[22] We first generated spin coherence by applying homogeneous magnetic field to the cell. After the delay time τ, we applied the control beam and generated the probe beam. Plotting the dependence of the probe intensity on the delay time τ and fitting it with exponentially decaying function, coherence time was estimated to be $146 \pm 7\ \mu$s.
[23] J. M. Vaughan and D. V. Willetts, Opt. Commun. **30**, 263 (1979).
[24] A. G. White, C. P. Smith, N. R. Heckenberg, H. Rubinsztein-Dunlop, R. Mcduff, C. O. Weiss, and C. Tamm, J. Mod. Opt. **38**, 2531 (1991).
[25] A. Vaziri, G. Weihs, and A. Zeilinger, J. Opt. B: Quantum Semiclassical Opt. **4**, S47 (2002).
[26] A. Mair, J. Hager, D. F. Phillips, R. L. Walsworth, and M. D. Lukin, Phys. Rev. A **65**, 031802(R) (2002).
[27] M. Kitagawa and M. Ueda, Phys. Rev. A **47**, 5138 (1993).
[28] H. Saito and M. Ueda, Phys. Rev. A **59**, 3959 (1999).
[29] U. V. Poulsen and K. Mølmer, Phys. Rev. Lett. **87**, 123601 (2001).